TẠP CHÍ KHOA HỌC
TRƯỜNG ĐẠI HỌC QUY NHƠN

Điều khiển các bộ điện tử công suất của máy phát điện không đồng bộ nguồn kép không chổi than sử dụng máy biến áp quay

Lê Thái Hiệp*, Nguyễn An Toàn

Khoa Kỹ thuật và Công nghệ, Trường Đại học Quy Nhơn, Việt Nam

Ngày nhận bài: 20/08/2021; Ngày nhận đăng: 01/11/2021

TÓM TẮT

Các loại máy phát điện không đồng bộ nguồn kép không chổi than (BDFIG) đã được chứng minh là giảm thiểu được chi phí bảo dưỡng và chi phí vận hành, trong khi lại tăng độ tin cậy so với máy phát điện không đồng bộ nguồn kép dùng trong điện gió. Bài báo này đã đề xuất phương pháp điều khiển các bộ điện tử công suất của máy phát điện không đồng bộ nguồn kép không chổi than sử dụng máy biến áp quay (BDFIG-RT) trong vai trò làm máy phát cho tuabin điện gió loại tốc độ thay đổi. Bộ điều khiển được đề xuất dựa trên hệ trục dq gắn trên rôto, và được mô phỏng trên phần mềm Matlab Simulink. Các kết quả mô phỏng cho thấy rằng đáp ứng động học hoàn toàn tốt trong trường hợp tốc độ gió thay đổi, kể cả có xảy ra sự cố ngắn mạch trên lưới. Nhờ phương pháp điều khiển này mà trong quá trình xảy ra ngắn mạch trên lưới thì máy phát vẫn kết nối với lưới và hoạt động ổn định.

Từ khóa: *Máy phát điện không đồng bộ nguồn kép không chổi than sử dụng máy biến áp quay, bộ biến đổi phía lưới, bộ biến đổi phía rôto, bộ điện tử công suất, máy biến áp quay.*

**Tác giả liên hệ chính.*
Email: lethaihiep@qnu.edu.vn

JOURNAL OF SCIENCE
QUY NHON UNIVERSITY

Control of power converters in the brushless doubly fed induction generator with rotary transformer

Le Thai Hiep*, Nguyen An Toan

Faculty of Engineering and Technology, Quy Nhon University, Vietnam

Received: 20/08/2021; Accepted: 01/11/2021

ABSTRACT

Brushless doubly fed induction generators (BDFIGs) show commercial promise for wind-power generation due to their lower capital and operational costs and higher reliability as compared with doubly fed induction generators. This paper proposed a control method of power converters in the brushless doubly fed induction generator with rotary transformer (BDFIG-RT), which operate as a variable-speed generator. The proposed controller is designed on the rotating dq reference frame, and simulated in Matlab Simulink. The simulation results show that the proposed controller has good dynamic performance when changes in wind speed and short circuit fault on grid. Thanks to this control system, the generator is still connected to the grid, and operates stably during a short circuit fault.

Keywords: *Brushless doubly fed induction generator with rotary transformer, grid-side converter, rotor-side converter, power converter, rotary transformer.*

1. INTRODUCTION

Currently, there are many types of wind generators, but the type of doubly fed induction generator (DFIG) is being used commonly. This type of generator is more popularly used due to the advantages of installation cost and wide wind energy exploitation range from 4 m/s to 24 m/s. This range is from less than 30% to over 30% of the synchronous speed, respectively. However, every DFIG needs to use carbon brushes to make electrical connections between the rotor windings and power supply from the power electronics. Using carbon brushes will cause sparks, contact resistance, wear of brushes and slip rings, heat generation at the point of contact, etc. These problems reduce the reliability of a DFIG. There are many methods of manufacturing Brushless Doubly Fed Induction Generators (BDFIGs). Particularly, they are divided into main groups:

- Unified BDFIG is in just one machine. This BDFIG type has two stators (the electrical parts and also the magnetic parts are separated) and a common rotor (the electrical parts are connected together, but the magnetic parts are separated).[1-4] Similar to this type is a brushless doubly-fed reluctance generator.[5] In these types, windings of a stator generating power are directly connected to the grid, but the windings of the other stator for control are connected to the grid through power electronics.[1-8]

- Another type of BDFIG is Brushless Doubly Fed Induction Generator with Rotary Transformer (BDFIG-RT). The main part of this type is DFIG. But instead of the three-phase

* *Corresponding author.*
Email: lethaihiep@qnu.edu.vn

https://doi.org/10.52111/qnjs.2022.16104

windings of the generator rotor are connected to the slip rings and carbon brushes, they are connected to the rotor windings of a three -phase rotating transformer. The stator windings of this transformer are powered by a power electronics unit.[1,9-12]

- A handful of BDFIGs are combinations of two blocks from two machines. This BDFIG type, stator windings of main generator are directly connected to the grid, and rotor windings of this generator are supplied by an auxiliary generator via a rotated inverter.[1,13] This auxiliary generator can be a wound rotor induction generator, the rotor windings connected to a rotated inverter.[13] Or the BDFIG type is formed from two wound rotor induction generators with their rotor parts connected both mechanically and electrically.[1,14]

Among the BDFIG types, the BDFIG-RT type has the simplest structure, very similar to the traditional DFIG type. Therefore, BDFIG-RT has the prospect of commercialization and application to replace DFIG in the near future.

There have been many studies on BDFIG-RT, but no detailed study focused on the control of this machine. Therefore, the purpose of this study is to analyze and propose control loops for the power converters of BDFIG-RT.

2. THE PROPOSED CONTROL STRUCTURES

2.1. Operational characteristics of the BDFIG-RT

The BDFIG type that uses a rotary transformer to supply electric power to the rotor windings (as shown in Figure 1). The generator stator windings in the BDFIG-RT are connected directly to the grid, but the generator rotor windings are connected to the rotor windings of a rotary transformer. Besides, the stator windings of this transformer are powered by a rotor-side converter (RSC) combined with a grid-side converter (GSC) connected to the grid (as shown in Figure 2). The rotary transformer is designed to be suitable for generators in the form (a) or the form (b) as shown in Figure 1.[9-12]

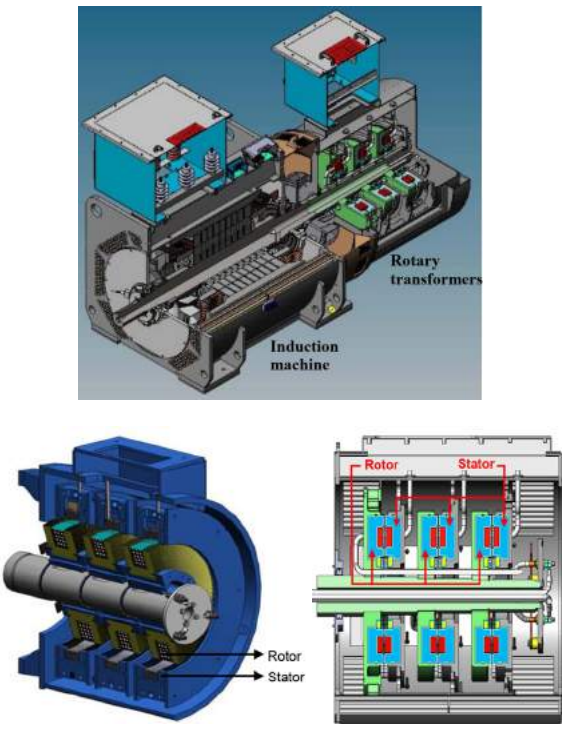

Figure 1. Sectional view of the BDFIG-RT structure, with either a rotary transformer of type (a) or type (b).[9-12]

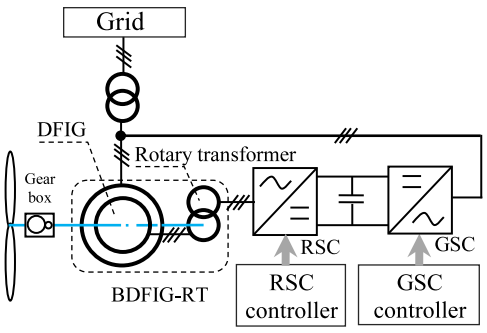

Figure 2. Electrical connection diagram in BDFIG-RT

The main part of BDFIG-RT is composed from DFIG, so it has the same power characteristics as DFIG. So BDFIG-RT can operate in sub- and super-synchronous modes, and there is also a synchronous mode in the short-term. Specifically, during operation, BDFIG-RT usually operates in two modes:

- When the rotor rotational speed is less than the synchronous speed of the stator magnetic field, the generator works in sub-synchronous mode. In this case, the rotation of the rotor magnetic field generated by the rotor currents is the same direction as the rotation of

the mechanical torque. So in this mode, rotor receives energy from the grid (Figure 3.a). With that, the GSC works as a rectifier and the RSC works as an inverter to generate rotor currents with an appropriate frequency. This frequency is suitable for the speed that needs to be supplemented with the rotational speed of magnetic poles of the rotor to equal the synchronous speed. In this mode, the generator rotor receives energy from the grid, only the generator stator generates power (Figure 4.a).

- Conversely, when the rotor rotates at a speed more than the synchronous speed of the stator magnetic field, the generator operates in super-synchronous mode. In this case, the rotation of the rotor magnetic field is opposite to the rotation of mechanical torque. So electricity is generated from the rotor to the grid (Figure 3.b). Then the RSC works as a rectifier and the GSC works as an inverter to generate currents with the same frequency as the grid frequency. In this mode, both stator and rotor sides of the generator supply active power to grid (Figure 4.c).

In the special case, when the rotor rotational speed is equal to the synchronous speed of the stator magnetic field, the generator works in synchronous mode. In which case, the rotor neither generates nor receives active power (Figure 4. b). But this mode only exists temporarily and is an intermediate mode in the above two modes, because the wind speed is always variable.

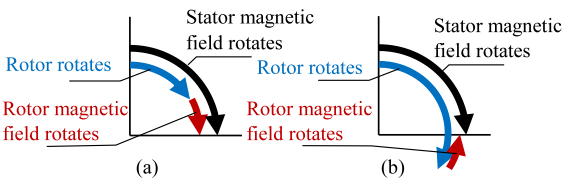

Figure 3. Direction and rotational speed of component magnetic fields and rotor speed in BDFIG-RT.

The active power generated in the stator (P_s) is calculated according to (1). The active power generated or received in the rotor (P_r) is calculated according to (2).

$$P_s = \frac{P_m}{1-s} \quad (1)$$

$$P_r = \frac{s}{1-s} P_m = sP_s \quad (2)$$

Where P_m is mechanical power.

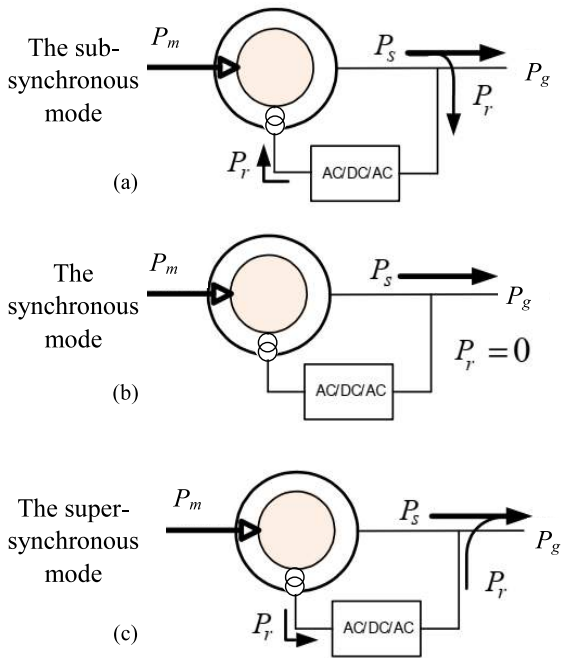

Figure 4. Power flows in BDFIG-RT.

With: $s = 1 - \frac{\omega}{\omega_s}$

Where: s is the slip ratio; ω_s is the speed of rotating magnetic field in the stator; ω is the rotational speed of the rotor.

2.2. Modeling BDFIG-RT

With a DFIG, the current and voltage can be measured in both stator and rotor sides. But the similar parameters can be only measured in the stator of the BDFIG-RT. The value of current and voltage in the rotor of this generator must be measured indirectly through the stator windings of the rotating transformer (Figure 5).

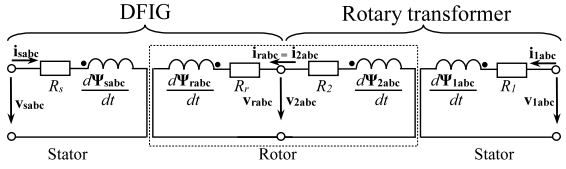

Figure 5. Single-phase equivalent circuit diagram of BDFIG-RT.

https://doi.org/10.52111/qnjs.2022.16104

The equations describe the relationship between voltage and other parameters in a DFIG:

$$\mathbf{v}_{\mathbf{sabc}} = R_s \mathbf{i}_{\mathbf{sabc}} + \frac{d\boldsymbol{\psi}_{\mathbf{sabc}}}{dt} \quad (3)$$

$$\mathbf{v}_{\mathbf{rabc}} = R_r \mathbf{i}_{\mathbf{rabc}} + \frac{d\boldsymbol{\psi}_{\mathbf{rabc}}}{dt} \quad (4)$$

$$\mathbf{v}_{\mathbf{1abc}} = R_1 \mathbf{i}_{\mathbf{1abc}} + \frac{d\boldsymbol{\psi}_{\mathbf{1abc}}}{dt} \quad (5)$$

$$\mathbf{v}_{\mathbf{2abc}} = -R_2 \mathbf{i}_{\mathbf{2abc}} + \frac{d\boldsymbol{\psi}_{\mathbf{2abc}}}{dt} \quad (6)$$

Where, the parameters of generator part: R_s and R_r are the stator and rotor resistance; $\mathbf{v}_{\mathbf{sabc}}$ and $\mathbf{v}_{\mathbf{rabc}}$ are the three-phase stator and rotor voltage matrix; $\mathbf{i}_{\mathbf{sabc}}$ and $\mathbf{i}_{\mathbf{rabc}}$ are the three-phase stator and rotor current matrix; $\boldsymbol{\psi}_{\mathbf{sabc}}$ and $\boldsymbol{\psi}_{\mathbf{rabc}}$ are the three-phase stator and rotor flux matrix. The parameters of rotary transformer part: R_1 and R_2 are the stator and rotor resistance; $\mathbf{v}_{\mathbf{1abc}}$ and $\mathbf{v}_{\mathbf{2abc}}$ are the three-phase stator and rotor voltage matrix; $\mathbf{i}_{\mathbf{1abc}}$ and $\mathbf{i}_{\mathbf{2abc}}$ are the three-phase stator and rotor current matrix; $\boldsymbol{\psi}_{\mathbf{1abc}}$ and $\boldsymbol{\psi}_{\mathbf{2abc}}$ are the three-phase stator and rotor flux matrix.

The rotary transformer rotor and the generator rotor are connected in the same phase with each other. Therefore, the current and voltage of the same phase of them are equal (as shown in Figure 5).

$$\mathbf{v}_{\mathbf{2abc}} = \mathbf{v}_{\mathbf{rabc}} \quad (7)$$

$$\mathbf{i}_{\mathbf{2abc}} = \mathbf{i}_{\mathbf{rabc}} \quad (8)$$

The flux in the stator of generator part is created by the inductance in the phases of the stator itself, plus the mutual inductance of the phases in the rotor to the stator. The same goes for the rotor of generator part. The phenomenon is similar for rotary transformer.

$$\boldsymbol{\psi}_{\mathbf{sabc}} = \boldsymbol{\psi}_{\mathbf{sabc(s)}} + \boldsymbol{\psi}_{\mathbf{sabc(r)}} \quad (9)$$

$$\boldsymbol{\psi}_{\mathbf{rabc}} = \boldsymbol{\psi}_{\mathbf{rabc(s)}} + \boldsymbol{\psi}_{\mathbf{rabc(r)}} \quad (10)$$

$$\boldsymbol{\psi}_{\mathbf{1abc}} = \boldsymbol{\psi}_{\mathbf{1abc(1)}} + \boldsymbol{\psi}_{\mathbf{1abc(2)}} \quad (11)$$

$$\boldsymbol{\psi}_{\mathbf{2abc}} = \boldsymbol{\psi}_{\mathbf{2abc(1)}} + \boldsymbol{\psi}_{\mathbf{2abc(2)}} \quad (12)$$

Where, $\boldsymbol{\psi}_{\mathbf{sabc(s)}}$, $\boldsymbol{\psi}_{\mathbf{rabc(r)}}$, $\boldsymbol{\psi}_{\mathbf{1abc(1)}}$, $\boldsymbol{\psi}_{\mathbf{2abc(2)}}$ are inductive flux components, and mutual inductance flux components include $\boldsymbol{\psi}_{\mathbf{sabc(r)}}$, $\boldsymbol{\psi}_{\mathbf{rabc(s)}}$, $\boldsymbol{\psi}_{\mathbf{1abc(2)}}$, $\boldsymbol{\psi}_{\mathbf{2abc(1)}}$.

In order to analyze the control process, it is necessary to convert the three-phase voltage, current, and magnetic flux parameters in the *abc* reference frame to the *dq* reference frame attached to the rotor. These parameters are converted according to the Park transition. The voltage equations (3)-(6) are rewritten in the *dq* reference frame:

$$\underline{v}_{sdq} = R_s \underline{i}_{sdq} + \frac{d\underline{\psi}_{sdq}}{dt} + j\omega_s \underline{\psi}_{sdq} \quad (13)$$

$$\underline{v}_{rdq} = R_r \underline{i}_{rdq} + \frac{d\underline{\psi}_{rdq}}{dt} + j\omega_{sl} \underline{\psi}_{rdq} \quad (14)$$

$$\underline{v}_{2dq} = -R_2 \underline{i}_{2dq} + \frac{d\underline{\psi}_{2dq}}{dt} + j\omega_{sl} \underline{\psi}_{2dq} \quad (15)$$

$$\underline{v}_{1dq} = R_1 \underline{i}_{1dq} + \frac{d\underline{\psi}_{1dq}}{dt} + j\omega_{sl} \underline{\psi}_{1dq} \quad (16)$$

With $\underline{i}_{rdq} = \underline{i}_{2dq}$, $\underline{v}_{rdq} = \underline{v}_{2dq}$.

Besides, $\omega_{sl} = \omega_s - \omega_r$ is the slip speed, which is also the rotational speed of the rotor magnetic field.

The stator and rotor fluxes of generator and rotary transformer can be written in the *dq* reference frame as follows:

$$\underline{\psi}_{sdq} = L_s \underline{i}_{sdq} + L_m \underline{i}_{rdq} \quad (17)$$

$$\underline{\psi}_{rdq} = L_m \underline{i}_{sdq} + L_r \underline{i}_{rdq} \quad (18)$$

$$\underline{\psi}_{1dq} = L_1 \underline{i}_{1dq} + L_{tm} \underline{i}_{2dq} \quad (19)$$

$$\underline{\psi}_{2dq} = L_{tm} \underline{i}_{1dq} + L_2 \underline{i}_{2dq} \quad (20)$$

Where

$$L_s = L_m + L_{s\sigma} \quad (21)$$

$$L_r = L_m + L_{r\sigma} \quad (22)$$

$$L_1 = L_{tm} + L_{1\sigma} \quad (23)$$

$$L_2 = L_{tm} + L_{2\sigma} \quad (24)$$

Where L_m is mutual inductance, L_s, $L_{s\sigma}$ are stator inductance and stator leakage inductance, L_r, $L_{r\sigma}$ are rotor inductance and rotor leakage inductance of generator part. Similarly, L_{tm} is mutual inductance, L_1, $L_{1\sigma}$ are stator inductance and stator leakage inductance, L_2, $L_{2\sigma}$ are rotor inductance and rotor leakage inductance of rotary transformer part.

The active and reactive power in the stator of the generator P_s, Q_s are calculated according to (25), (26). Likewise, the active and reactive power in the stator of the rotary transformer P_1, Q_1 are calculated by equations (27), (28), respectively.

$$P_s = \frac{3}{2}\mathrm{Re}\left\{\underline{v}_{sdq}\hat{\underline{i}}_{sdq}\right\} = \frac{3}{2}\left(v_{sd}i_{sd} + v_{sq}i_{sq}\right) \quad (25)$$

$$Q_s = \frac{3}{2}\mathrm{Im}\left\{\underline{v}_{sdq}\hat{\underline{i}}_{sdq}\right\} = \frac{3}{2}\left(v_{sq}i_{sd} - v_{sd}i_{sq}\right) \quad (26)$$

$$P_1 = \frac{3}{2}\mathrm{Re}\left\{\underline{v}_{1dq}\hat{\underline{i}}_{1dq}\right\} = \frac{3}{2}\left(v_{1d}i_{1d} + v_{1q}i_{1q}\right) \quad (27)$$

$$Q_1 = \frac{3}{2}\mathrm{Im}\left\{\underline{v}_{1dq}\hat{\underline{i}}_{1dq}\right\} = \frac{3}{2}\left(v_{1q}i_{1d} - v_{1d}i_{1q}\right) \quad (28)$$

Where $\hat{\underline{i}}_{sdq}$ and $\hat{\underline{i}}_{1dq}$ are complex conjugate $\underline{i}_{sdq}$ and $\underline{i}_{1dq}$.

2.3. Model and propose control loops of GSC connected to an inductive filter

In the circuit shown in Figure 6, R_g is the resistance of the filter reactor L_g.

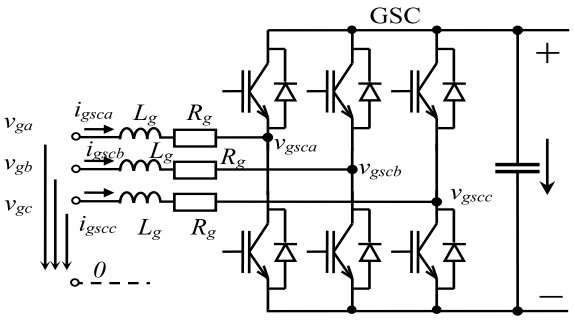

Figure 6. The GSC connected to an three-phase inductive filter.

On the basis of the circuit shown in Figure 6, the voltage matrix on the grid is calculated:

$$\mathbf{v}_{\mathbf{gabc}} = L_g\frac{d\mathbf{i}_{\mathbf{gscabc}}}{dt} + R_g\mathbf{i}_{\mathbf{gscabc}} + \mathbf{v}_{\mathbf{gscabc}} \quad (29)$$

Convert (29) to the dq reference frame with the d axis coincident with the grid voltage vector, and this reference frame rotates at synchronous speed.

$$\underline{v}_{gdq} = L_g\frac{d\underline{i}_{gscdq}}{dt} + R_g\underline{i}_{gscdq} + j\omega_s L\underline{i}_{gscdq} + \underline{v}_{gscdq} \quad (30)$$

The power that is received from the grid into the GSC is determined as follows:

$$P_{gsc} = -\frac{3}{2}\mathrm{Re}\left\{\underline{v}_{gdq}\hat{\underline{i}}_{gscdq}\right\} = -\frac{3}{2}\left(v_{gd}i_{gscd} + v_{gq}i_{gscq}\right) \quad (31)$$

$$Q_{gsc} = -\frac{3}{2}\mathrm{Im}\left\{\underline{v}_{gdq}\hat{\underline{i}}_{gscdq}\right\} = -\frac{3}{2}\left(v_{gq}i_{gscd} - v_{gd}i_{gscq}\right) \quad (32)$$

Where $\hat{\underline{i}}_{gscdq}$ is complex conjugate of $\underline{i}_{gscdq}$.

From equation (29), a control loop for the GSC set in the Laplace is determined as follows:

$$\underline{v}_{gscdq} = \underline{v}_{gdq} - \underline{v}^*_{gscdq} - j\omega_s L\underline{i}_{gscdq} \quad (33)$$

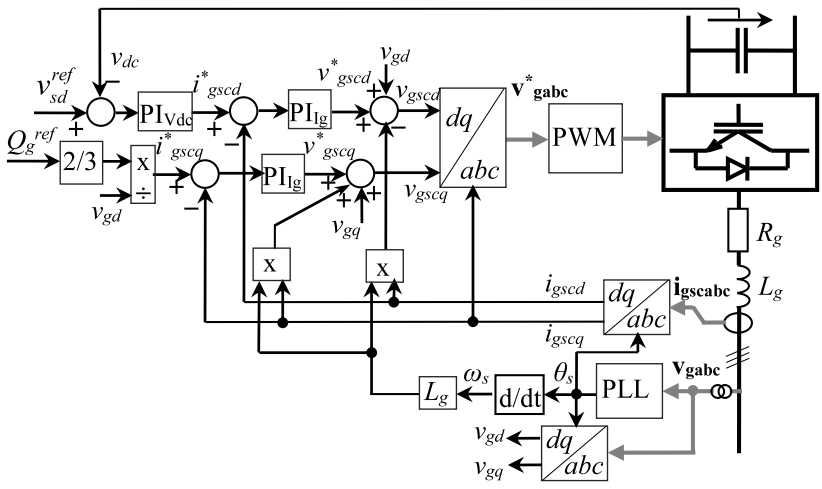

Figure 7. Control diagram of GSC.

https://doi.org/10.52111/qnjs.2022.16104

With $\underline{v}^*_{gscdq} = (L_g s + R_g)\underline{i}_{gscdq}$

Where $\underline{v}^*_{gscdq}$ is determined from the current control loop $\underline{i}_{gscdq}$ with the PI_{Ig} regulator.

$$\underline{v}^*_{gscdq} = \left(k_{pIg} + \frac{k_{iIg}}{s}\right)(\underline{i}^*_{gscdq} - \underline{i}_{gscdq}) \quad (34)$$

Where $\underline{i}_{gscdq}$ is determined from the DC voltage control loop v_{dc} with the PI_{Vdc} controller.

$$i^*_{gscd} = \left(k_{pVdc} + \frac{k_{iVdc}}{s}\right)(v^{ref}_{dc} - v_{dc}) \quad (35)$$

With v^{ref}_{dc} is the DC voltage setting value in the GSC and RSC.

And i^*_{gscd} is determined through reactive power setting value (Q^{ref}_{gsc}) at the GSC:

$$i^*_{gscq} = \frac{2}{3}\frac{Q^{ref}_{gsc}}{v_{gd}} \quad (36)$$

From equations (33)-(36), this study has established the control diagram for the GSC as shown in Figure 7.

2.4. Propose RSC control loops

From equation (18), $\underline{i}_{rdq}$ can be determined:

$$\underline{i}_{rdq} = \frac{1}{L_m}\underline{\psi}_{sdq} - \frac{L_s}{L_m}\underline{i}_{sdq} \quad (37)$$

Substitute (37) into the equation (19) to get:

$$\underline{\psi}_{1dq} = L_1\underline{i}_{1dq} + \frac{L_{tm}}{L_m}\underline{\psi}_{sdq} - \frac{L_{tm}L_s}{L_m}\underline{i}_{sdq} \quad (38)$$

Then, substitute (38) into the equation (16) to get:

$$\underline{v}_{1dq} = R_1\underline{i}_{1dq} + \frac{d}{dt}\left(L_1\underline{i}_{1dq} + \frac{L_{tm}}{L_m}\underline{\psi}_{sdq} - \frac{L_{tm}L_s}{L_m}\underline{i}_{sdq}\right) + j\omega_{sl}\left(L_1\underline{i}_{1dq} + \frac{L_{tm}}{L_m}\underline{\psi}_{sdq} - \frac{L_{tm}L_s}{L_m}\underline{i}_{sdq}\right) \quad (39)$$

Convert equation (39) into the Laplace:

$$\underline{v}_{1dq} = \underline{v}^*_{I1dq} + \underline{v}^*_{\psi sdq} - \underline{v}^*_{Isdq} + j\omega_{sl}\left(L_1\underline{i}_{1dq} + \frac{L_{tm}}{L_m}\underline{\psi}_{sdq} - \frac{L_{tm}L_s}{L_m}\underline{i}_{sdq}\right) \quad (40)$$

With: $\underline{v}^*_{I1dq} = (R_1 + L_1 s)\underline{i}_{1dq}$, $\underline{v}^*_{Isdq} = \frac{L_{tm}L_s}{L_m}s\underline{i}_{sdq}$, $\underline{v}^*_{\psi sdq} = \frac{L_{tm}}{L_m}s\underline{\psi}_{sdq}$.

Where: $\underline{v}^*_{I1dq}$ is determined from the current control loop $\underline{i}_{1dq}$ with the PI_{I1} regulator; $\underline{v}^*_{Isdq}$ is determined from current control loop $\underline{i}_{sdq}$ with the PI_{Is} regulator; $\underline{v}^*_{\psi sdq}$ is determined from the magnetic flux control loop $\underline{\psi}_{sdq}$ with the regulator $PI_{\psi s}$.

$$\underline{v}^*_{I1dq} = \left(k_{pI1} + \frac{k_{iI1}}{s}\right)(\underline{i}^*_{1dq} - \underline{i}_{1dq}) \quad (41)$$

$$\underline{v}^*_{Isdq} = \left(k_{pIs} + \frac{k_{iIs}}{s}\right)(\underline{i}^*_{sdq} - \underline{i}_{sdq}) \quad (42)$$

$$\underline{v}^*_{\psi sdq} = \left(k_{p\psi s} + \frac{k_{i\psi s}}{s}\right)(\underline{\psi}^*_{sdq} - \underline{\psi}_{sdq}) \quad (43)$$

From equations (25), (26), they are combined with $v^{ref}_{sq} = 0$, $v^{ref}_{sd} = v^{ref}_s$, (because the *dq* reference frame is attached to the rotor, with the d-axis is the same direction as the stator voltage vector, and this reference frame rotates at synchronous speed ω_s), leading to i^*_{sd} and i^*_{sq} ; and are determined:

$$i^*_{sd} = \frac{2}{3}\frac{P_s}{v^{ref}_{sd}} \quad (44)$$

$$i^*_{sq} = -\frac{2}{3}\frac{Q_s}{v^{ref}_{sd}} \quad (45)$$

Transient fluctuations of stator flux in the *dq* reference frame can be ignored when determining a reference value, so the equation (13) is rewritten:

$$\underline{v}^{ref}_{sdq} \approx R_s\underline{i}^*_{sdq} + j\omega_s\underline{\psi}^*_{sdq} \quad (46)$$

From (46), ψ^*_{sd}, ψ^*_{sq} are determined:

$$\psi^*_{sd} \approx -\frac{R_s i^*_{sq}}{\omega_s} \quad (47)$$

$$\psi^*_{sq} \approx \frac{R_s i^*_{sd}}{\omega_s} - \frac{v^{ref}_{sd}}{\omega_s} \quad (48)$$

To determine according to the torque control method (corresponding to the active power), it can be based on the electromagnetic torque of the DFIG:

$$T_e = \frac{3}{2}(\psi_{sd}i_{sq} - \psi_{sq}i_{sd}) \approx -\frac{3}{2}\psi_{sq}i_{sd} \quad (49)$$

With $\psi_{sd} = L_s i_{sd} + L_m i_{rd} \approx 0$

Therefore $i_{sd} \approx -\frac{L_m}{L_s} i_{rd}$

Thanks to that, from (49) can determine i_{rd}:

$$i_{rd} \approx \frac{2}{3} \frac{L_s T_e}{L_m \psi_{sq}} \quad (50)$$

If the power losses on the windings and steel cores of the rotary transformer are neglected, the power transmitted through the windings of the rotating transformer can be considered to be approximately equal.

$$\frac{3}{2}\left(v_{1d} i_{1d} + v_{1q} i_{1q}\right) \approx \frac{3}{2}\left(v_{2d} i_{2d} + v_{2q} i_{2q}\right) \quad (51)$$

Thus, $v_{1d} i_{1d} \approx v_{2d} i_{2d}$, $v_{1q} i_{1q} \approx v_{2q} i_{2q}$.

Thereby, i_{1d}^* can be determined based on combination with the equation (50) and $\underline{i}_{2dq} = \underline{i}_{rdq}$:

$$i_{1d}^* \approx \frac{i_{rd}}{k_t} \approx \frac{2}{3} \frac{L_s T_e^{ref}}{k_t L_m \psi_{sq}} \quad (52)$$

Where $k_t = v_1/v_2$ is the voltage variation ratio of rotary transformer; the torque T_e^{ref} is determined by looking up the wind turbine characteristics corresponding to the rotor rotation speed.

From equation (17), i_{sq} is determined:

$$i_{sq} = \frac{1}{L_s} \psi_{sq} - \frac{L_m}{L_s} i_{rq} \quad (53)$$

Equation (48) and equation (53) are combined together, and if the stator resistance is ignored, then i_{sq} is determined as follows:

$$i_{sq} \approx -\frac{v_{sd}}{\omega_s L_s} - \frac{L_m}{L_s} i_{rq} \quad (54)$$

From (26) is combined with (54), $v_{sq}^{ref} = 0$, $v_{sd}^{ref} = v_s^{ref}$, it is rewritten as below:

$$Q_s \approx -\frac{3}{2} v_{sd}^{ref} i_{sq} \approx \frac{3}{2} \frac{(v_{sd}^{ref})^2}{\omega_s L_s} + \frac{3}{2} \frac{L_m}{L_s} v_{sd}^{ref} i_{rq} \quad (55)$$

Thanks to (55) combined with $\underline{i}_{2dq} = \underline{i}_{rdq}$, i_{1q}^* can be determined as follows:

$$i_{1q}^* \approx \frac{i_{2q}}{k_t} \approx \frac{2}{3} \frac{L_s Q_s}{k_t L_m v_{sd}^{ref}} - \frac{v_{sd}^{ref}}{k_t \omega_s L_m} \quad (56)$$

On the basis of equation (40) combined with other mathematical expressions presented above, the RSC control diagram is proposed as shown in Figure 8.

3. SIMULATION

3.1. The simulated system

In order to check the operation of the control system proposed above, an application of BDFIG-RT in the power grid with the structure shown in Figure 9 is simulated in this study. Due to the generator is an asynchronous generator, it is usually consumed a large amount of reactive power. Therefore, the generator is usually connected with a three-phase compensator capacitor to directly supply a basic amount of reactive power to it (Figure 9.a). In addition, for the purpose of converting the characteristics of generator from a DFIG to a wound-rotor asynchronous generator connected the auxiliary resistor, an auxiliary resistor (R_crowbar) is connected to the stator of the rotating transformer (Figure 9.a).[15] As a result, the generator can be still connected to the grid in a certain time when there is a short circuit fault on the grid.[15]

https://doi.org/10.52111/qnjs.2022.16104

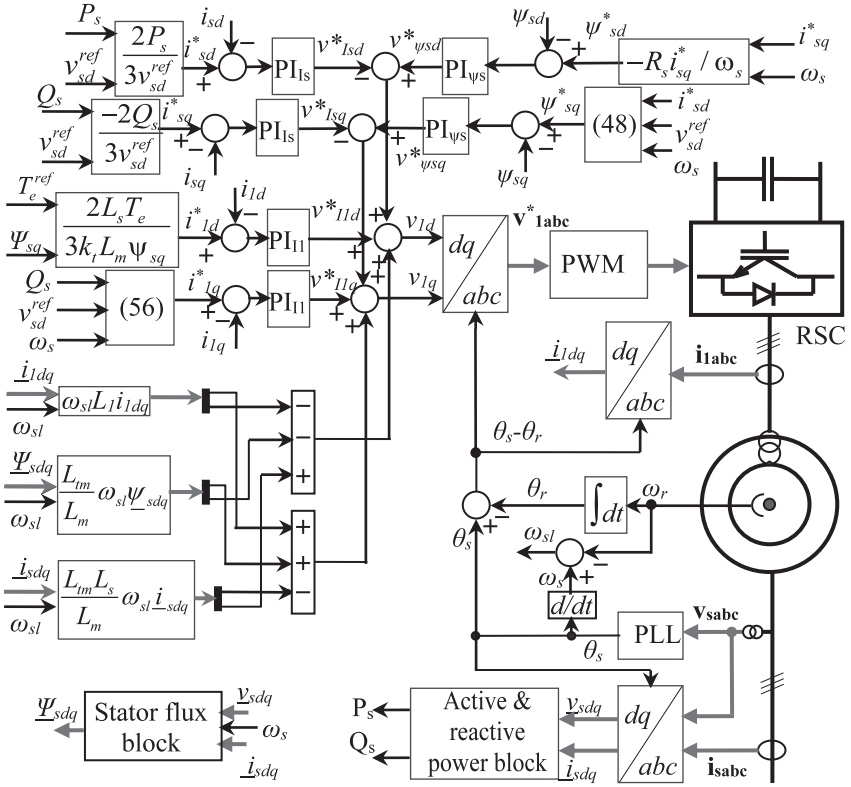

Figure 8. Control diagram of RSC

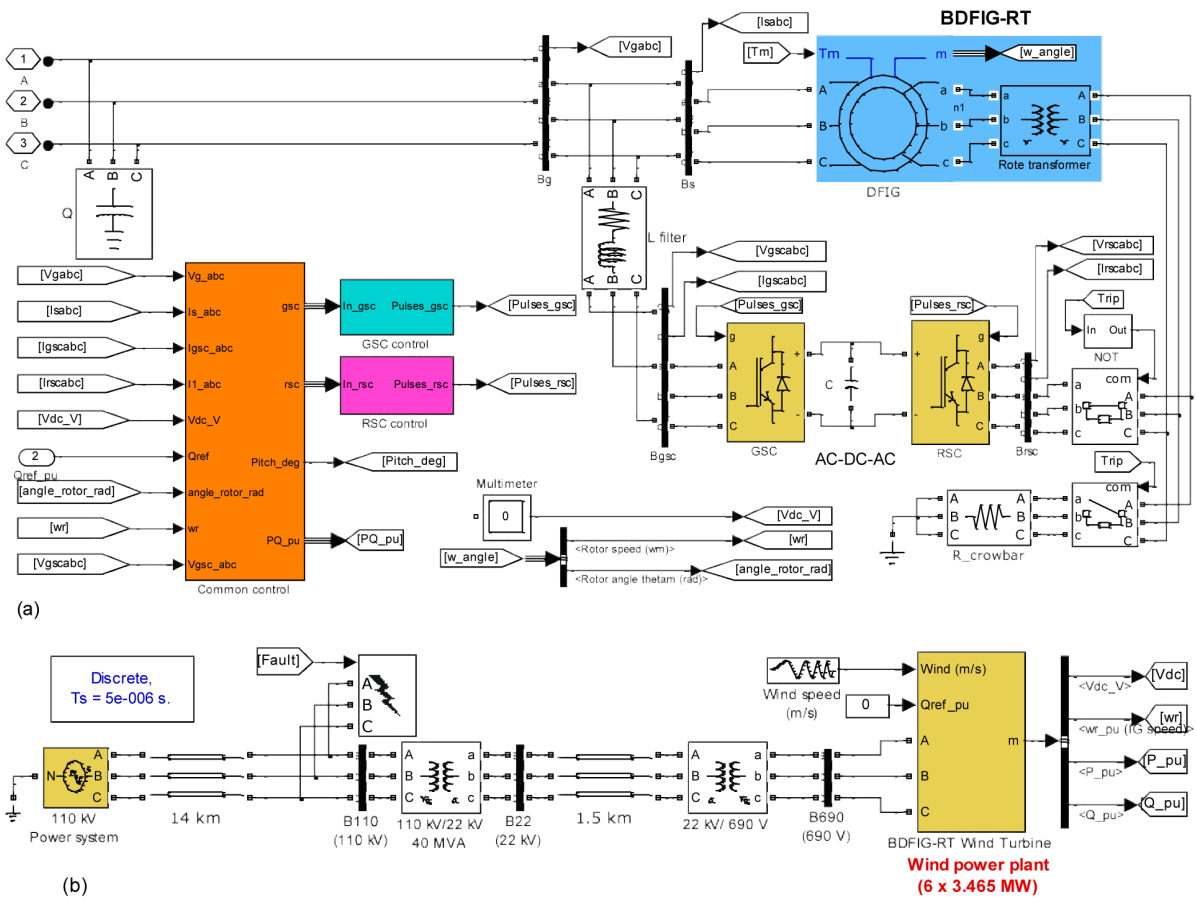

Figure 9. The structure of BDFIG-RT (a), and it is connected to the grid (b) in Matlab Simulink

The output voltage of each generator in the wind power plant is 690 V. This output is connected to a transformer to boost voltage from 690 V to 22 kV at each wind turbine. Next, the output of all transformers are connected together at a busbar in the 22kV/110kV power station (Figure 9.b). At this power station, the wind power plant is connected to the 110 kV power grid of the area.

3.2. Parameters of simulated system

The parameters of components of the wind power system using BDFIG-RT are presented in Table 1 – Table 3. In which, the wind turbine part (with parameters as Table 1) provides mechanical energy to the generator (with parameters as Table 2). The BDFIG-RT has the stator windings of the rotary transformer connected to the back-to-back power converter (with parameters as Table 3). This converter is connected to the grid via a three-phase filter inductor (with parameters as Table 3).

Table 1. Wind turbine parameters

Parameter	Value	Unit
Rated wind speed	12	m/s
Wind turbine inertia constant	3.32	s
Shaft mutual damping	0.75	pu
Shaft spring constant refer to high-speed shaft	1.11	pu

Table 2. BDFIG-RT parameters in the simulation

Parameter	Value	Unit
Generator data		
Rated power	3.465	MW
Rated stator voltage	690	V
Rated rotor voltage	1975	V
R_s (stator resistance)	0.023	pu
$L_{s\sigma}$ (stator leakage inductance)	0.18	pu
R_r (rotor resistance)	0.016	pu
$L_{r\sigma}$ (rotor leakage inductance)	0.16	pu
L_m (mutual inductance)	2.9	pu
Inertia constant	0.685	s
Pairs of poles	3	
Rotary transformer data		
Rated stator voltage	690	V
Rated rotor voltage	1975	V
R_1 (stator resistance)	0.1005	pu
$L_{1\sigma}$ (stator leakage inductance)	0.0022	pu
R_2 (rotor resistance)	0.0899	pu
$L_{2\sigma}$ (rotor leakage inductance)	0.0023	pu
L_{tm} (mutual inductance)	0.0545	pu

Table 3. Parameters of back-to-back power converter and filter inductor

Parameter	Value	Unit
v_{dc} (DC voltage)	1150	V
L_g (inductance of filter inductor)	0.3	pu
R_g (resistance of filter inductor)	0.003	pu

4. RESULTS AND DISCUSSION

Some different cases are simulated in this paper in order to check the suitability of the control system proposed above. First, it is the case of variable wind speed, the dynamic response of this system is examined. Second, this system is surveyed when there is a short circuit fault on the grid.

4.1. Case of variable wind speed

In this section, the operation of the system is simulated and considered when wind speed varies (as shown in Figure 10). The results of simulation shown that the generator speed varies within the appropriate range. This range is from less to over than 30% of the synchronous speed (Fig. 11.a). As a result, the variation of active power that is generated or received in the generator rotor via the rotary transformer is suitable for the control law presented (Figure 11.b). The active power that is generated in stator of the generator also varies dependently wind speed (Figure 11.b).

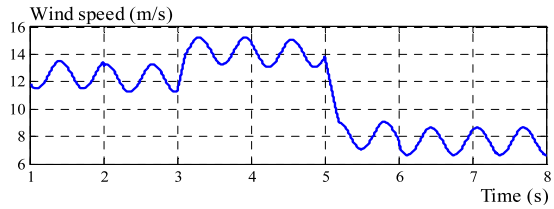

Figure 10. Wind speed chart.

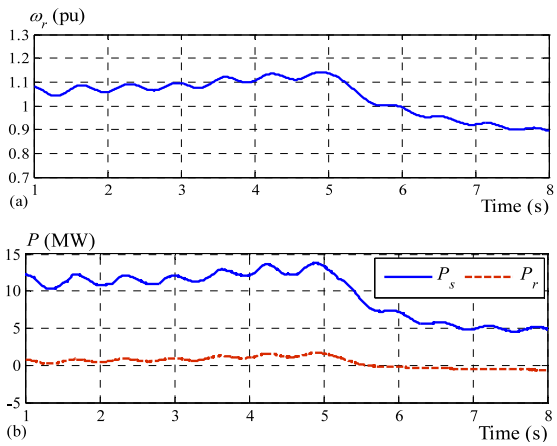

Figure 11. Chart of speed (a) and active power (b) of BDFIG-RT.

https://doi.org/10.52111/qnjs.2022.16104

4.2. Case of short circuit fault on the grid

The 1st case study: there was a three-phase short circuit fault on the 110 kV transmission grid and near the wind power plant. This fault has happened at 1.3 s, and it has been cleared at 1.45 s. The fault duration time was 150 ms, and the voltage has dropped to about 17.33% of the rated voltage during the this fault (as shown in Figure 12). The simulation results are shown in Figure 13 and Figure 14. According to the results in Figure 13, the control system has taken less than a current cycle to regulate the short-circuit current value to the permissible value (Figure 13.d). This control method has been based on the principle of converting the generator from a DFIG to a wound-rotor asynchronous generator connected the auxiliary resistors. According to this method, the active power that has been generated in the generator stator has been reduced to a minimum throughout the time of short circuit fault (as shown in Figure 13.a). Thereby, the overall power flow transfer to the grid has been reduced during the short circuit as shown in Figure 14.a. In the time of short circuit fault, the RSC has been controlled to neither transmit nor receive active power, this has been shown by the currents shown in Figure 13.b. For the purpose of stabilizing the voltage, the GSC has supplied reactive power into the grid (Figure 13.c). In addition, in order to recover the voltage after the fault, a large amount of reactive power has been supplied into the grid immediately after the short circuit fault has been cleared (Figure 14.b). Thanks to good control, the generator speed has been only slightly increased (as shown in Figure 14.c).

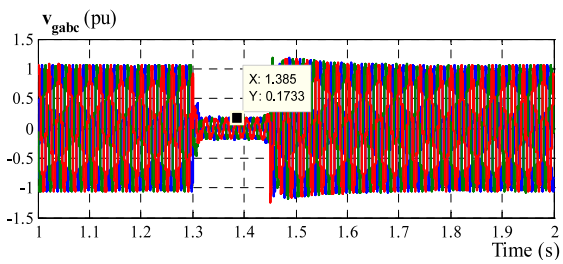

Figure 12. The grid voltage with 1st case study.

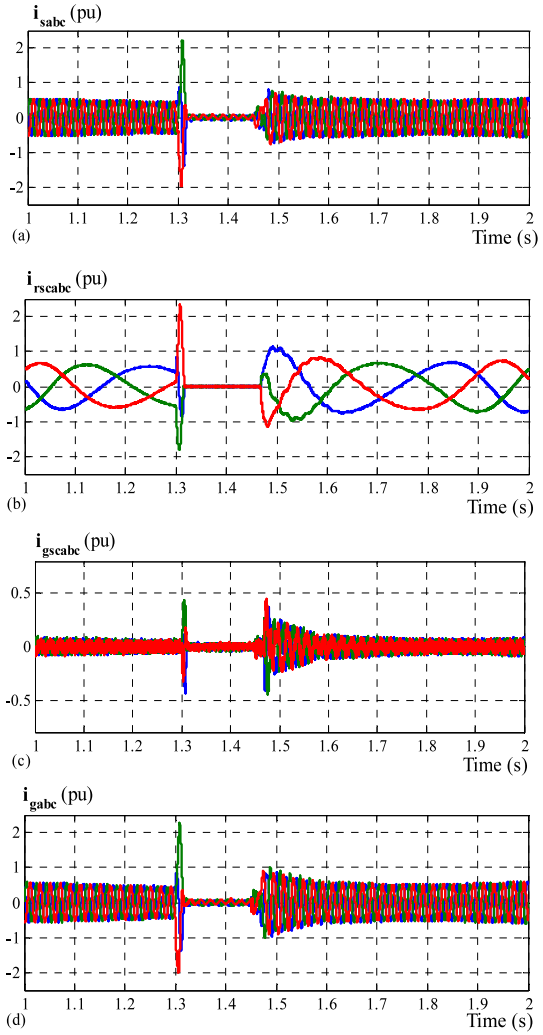

Figure 13. Currents in *abc* reference frame with 1st case study.

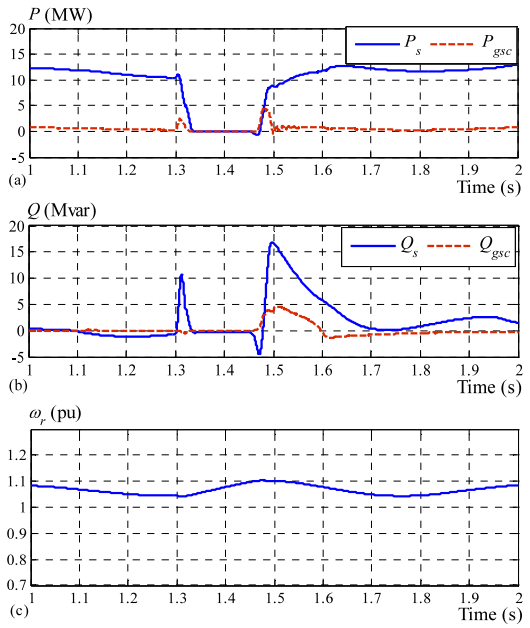

Figure 14. Power and speed of BDFIG-RT with 1st case study.

https://doi.org/10.52111/qnjs.2022.16104

The 2nd case study: there was a single phase-to-ground fault (C phase to ground) on the 110 kV transmission grid and near the wind power plant. This fault has happened at 1.3 s and has been cleared at 1.45 s. During the fault, the phase C voltage has dropped to about 19.55% of the rated value (Figure 15). At the same time, an overvoltage has occurred in the remaining 2 phases to about 1.33 pu (Figure 15). This value is smaller than the limited ground fault of 1.4 in the Circular No. 25/2016/TT-BCT of the Ministry of Industry and Trade. The simulation results of this case are shown in Figure 16 and Figure 17. According to the results in Figure 16, the control system has regulated the short-circuit currents within the normal operating range (Figure 16.d). In this case, the control method has not changed, even though the short circuit has been asymmetrical. In the time of short circuit fault, according to this method, the currents in the generator stator have been reduced (Figure 16.a). Therefore, the active power that has been generated by the generator has been reduced during the short circuit fault (Figure 17.a). In order to support voltage stability, the GSC (with a small contribution) together with the generator stator have consumed the reactive power of the grid (Figure 16.c and Figure 17.b). After that, the voltage of the grid has been reduced as soon as the fault has been cleared (Figure 15). Then, a large amount reactive power has been supplied by generator into the grid to support voltage stabilization at this time (Figure 17.b). During the short circuit fault, the RSC has been disabled (Figure 16.b). Thanks to the appropriate control, the generator speed has been increased only slightly (as shown in Figure 17.c).

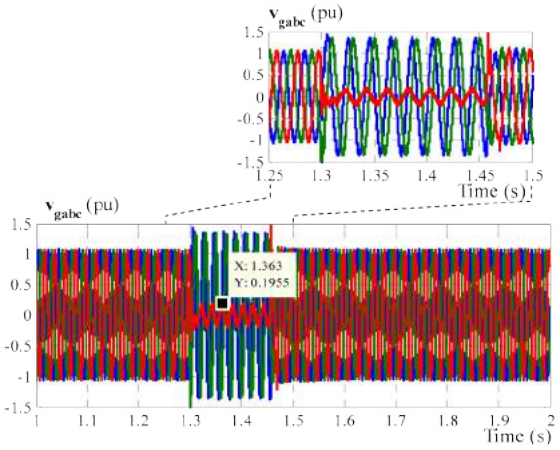

Figure 15. The grid voltage with 2nd case study.

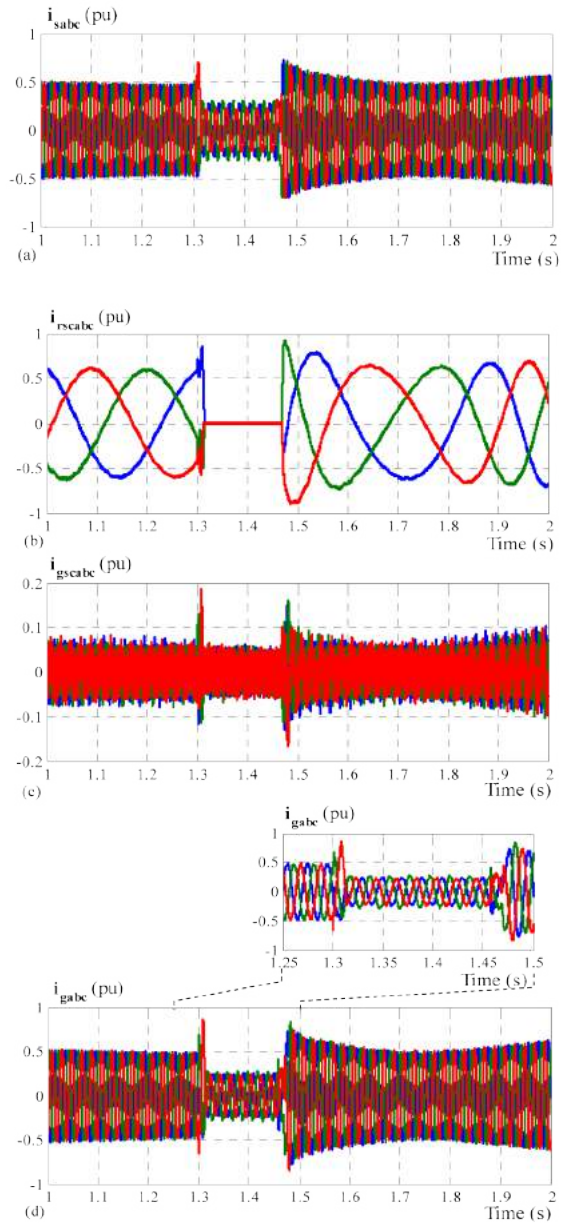

Figure 16. Currents in *abc* reference frame with 2nd case study.

https://doi.org/10.52111/qnjs.2022.16104

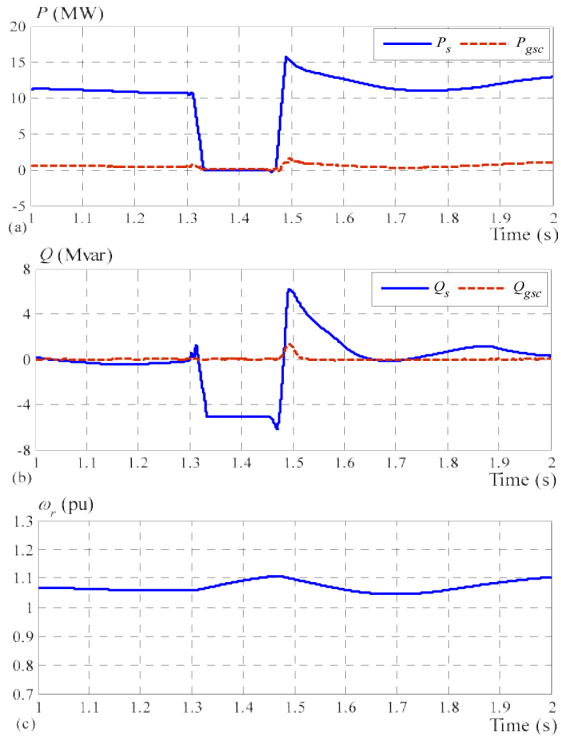

Figure 17. Power and speed of BDFIG-RT with 2nd case study.

Thus, through checking the dynamic process in the above cases, the control system proposed above has operated stably. The response time of the system was very short. Current and voltage parameters have conformed to the required values.

4. CONCLUSION

BDFIG-RTs solve the restrictions of DFIGs, which must be done maintenance of carbon brushes and slip rings, in wind power. This paper analyzed and proposed control loops for the power converters of a BDFIG-RT. This paper analyzed and proposed control loops for the power converters of BDFIG-RT. Through simulation in MatLab software, this research tested the proposed control loops. The simulation results of the system with a wind power station using BDFIG-RT showed that the operation of this system was stable with varying wind speed or a short circuit fault on the grid.

The results of this study serve as a premise for experimental studies and practical applications of BDFIG-RT in wind power.

Acknowledgment

This study is conducted within the framework of science and technology projects at institutional level of Quy Nhon University under project code T2020.670.18.

REFERENCES

1. M. Cheng, P. Han, G. Buja, M. G. Jovanović. Emerging multiport electrical machines and systems: Past developments, current challenges, and future prospects, *IEEE Transaction on Industrial Electronics*, **2018**, *65*(7), 5422 – 5435.
2. P. Han, M. Cheng, Y. Jiang and Z. Chen. Torque/power density optimization of a dual-stator brushless doubly-fed induction generator for wind power application, *IEEE Transaction on Industrial Electronics*, **2017**, *64*(12), 9864-9875.
3. H. Liu, Y. Zhang, F. Zhang, S. Jin, H. Zhang, H. Nian. Design and performance analysis of dual-stator brushless doubly-fed machine with cage-barrier rôtor, *IEEE Transactions on Energy Conversion*, **2019**, *34*(3), 1347 – 1357.
4. P. Han, M. Cheng, R. Luo. Design and analysis of a brushless doubly-fed induction machine with dual-stator structure, *IEEE Transactions on Energy Conversion*, **2016**, *31*(3), 1132 – 1141.
5. Min-Fu Hsieh, Yao-Hsin Chang, David G. Dorrell. Design and analysis of brushless doubly-fed reluctance machine for renewable energy applications, *IEEE Transactions on Magnetics*, **2016**, *52*(7).
6. S. Shao, E. Abdi, F. Barati, R. McMahon. Stator-flux-oriented vector control for brushless doubly fed induction generator, *IEEE Transaction on Industrial Electronics*, **2009**, *56*(10), 4220-4228.
7. R. Zhao, A. Zhang, Y. Ma, X. Wang, J. Yan, Z. Ma. The dynamic control of reactive power for the brushless doubly fed induction machine with indirect stator-quantities control scheme, *IEEE Transactions on Power Electronics,* **2015**, *30*(9), 5046 - 5057.
8. T. Taluo, L. Ristić, M. Jovanović. Dynamic modeling and control of BDFRG under

unbalanced grid conditions, *Energies,* **2021**, *14*(14), 1-25.

9. M. Ruviaro, F. Rüncos, N. Sadowski, I. M. Borges. Analysis and test results of a brushless doubly fed induction machine with rotary transformer*, IEEE Transaction on Industrial Electronics,* **2012**, *59*(6), 2670-2677.

10. M. Ruviaro, F. Rüncos. A brushless doubly fed induction machine with flat plane rotary transformers, *2012 XXth International Conference on Electrical Machines, IEEE*, 23-29, 2012.

11. M. Ruviaro, F. Rüncos. Wound rôtor doubly fed induction machine with radial rotary transformer, *Journal of Microwaves, Optoelectronics and Electromagnetic Applications*, **2013**, *12*(2), 411-426.

12. Hui Zhong, Chao Wu, Yingjie Wang. Design study on novel three-phase rotary transformer used for brushless doubly fed induction generators, *2017 20th International Conference on Electrical Machines and Systems (ICEMS), IEEE*, 1-5, 2017.

13. Naveed-ur-Rehman Malik, Chandur Sadarangani. Dynamic modeling and control of a brushless doubly-fed induction generator with a rotating power electronic converter, *2012 XXth International Conference on Electrical Machines, IEEE*, 900-906, 2012.

14. J. Hu, J. Zhu, D. G. Dorrell. A new control method of cascaded brushless doubly fed induction generators using direct power control, *IEEE Transactions on Energy Conversion*, **2014**, *29*(3), 771 - 779.

15. Tran Duong Hoang Phuc, Le Thai Hiep. Study on operating modes of doubly fed induction generator with a short circuit fault on grid near the wind power plant, *Journal of science – Quy Nhon university*, **2021**, *15*(1), 37-44.

https://doi.org/10.52111/qnjs.2022.16104